Journal of Computer Science and Technology Studies
ISSN: 2709-104X
DOI: 10.32996/jcsts
Journal Homepage: www.al-kindipublisher.com/index.php/jcsts

JCSTS
AL-KINDI CENTER FOR RESEARCH AND DEVELOPMENT

| RESEARCH ARTICLE

Efficiency Investigation and Modeling of an Ultra Thin-film CIGS Solar Cell using WxAMPS

Kashfi Barua Riea[1] ✉ and Rocky Chakma[2]
[12]Department of Electrical and Electronic Engineering, University of Science and Technology Chittagong, Chattogram- 4202, Bangladesh
Corresponding Author: Kashfi Barua Riea, **E-mail**: kashfibarua10338@gmail.com

| ABSTRACT
The highly efficient CIGS thin-film solar cell is numerically investigated in this paper using solar simulator software wxAMPS (Analysis of Microelectronic and Photonic Structures). WxAMPS is a customized simulation software package mainly used for photovoltaic cells, which supports quick data input and enhanced visualization with its improved user interface. Copper–indium–gallium–diselenide Cu(In, Ga)Se2 (CIGS) is a semiconductor material with chalcopyrite crystal structure that has high conversion efficiency and structural stability. CIGS model- ZnO: Al/ZnO/CdS/CIGS/Mo/substrate is mainly experimental research that considers the physical characteristics, dimensions, and thicknesses of the different layers. The bilayer window and absorber layer with different thicknesses are the critical factors that influence solar cell performance. The bilayer window concept can assist in reducing the loss at the window layer. In this paper, through the numerical simulation, the highest conversion efficiency was achieved, 18.7%, with an optimum bandgap of 1.12 eV with 3000 nm thickness of the absorber layer under AM 1.5G.

| KEYWORDS

Thin film, thickness, wxAMPS.

| ARTICLE INFORMATION

ACCEPTED: 01 October 2024 **PUBLISHED:** 16 October 2024 **DOI:** 10.32996/jcsts.2024.6.4.13

1. Introduction

Solar energy demand is increasing as green renewable energy has been used in recent days to fulfill electricity demand. Photovoltaic modules and solar thermal collectors are used in active solar technology. Photovoltaic technology is the direct method of solar electric technologies that produce energy by converting solar radiation directly into electricity through the photovoltaic effect [Solar Electric Technology, n.d]. The solar generation rate is about 5.52% in the year 2023 worldwide [Global Solar Energy, n.d]. Due to the highly intensive energy requirement in the process of manufacturing bulk silicon solar cells, copper indium gallium selenide (CIGS) is a great alternative as second generation thin-film solar cell technology that is 300 times smaller than that of traditional silicon solar cells [Columbus, 2014] [Solar Reviews, n.d]. CIGS modules are usually yielded by co-evaporation or co-deposition. Copper, Indium, Gallium, and Selenide are deposited onto the substrate at different temperatures to mix together [Thin-film Solar Cell, n.d]. Several researchers reported that CIGS solar cells represent lateral inhomogeneity on the μm range scale due to the local band splitting of quasi Fermi levels, which causes some effects on main parameters [Thin film solar, 2018] [Ahamed, 2017]. CIGS cells have several advantages over conventional solar cells, including being completely versatile, extremely lightweight, economical, and having fine stability. Furthermore, in CIGS solar cells, the open-circuit voltage can be enhanced by minimizing the number of cells arranged in series at the panel and, thus, lack of interconnection [Witte, 2012]. CIGS properties include band gap (Eg), lifetime, carrier density, mobility, and front and rear surface recombination velocities (SF and SR) that are considered to influence the device efficiency, which change from one thin film to another. Through the film, the gradient of the properties can appear [Antonino, 2015]. CIGS material has a high absorption coefficient, which is about $3 - 6 \times 10^5 cm^{-1}$ used as the absorber layer that can absorb more than 90% of sunlight at 1μm. It is a p-type polycrystalline semiconductor material with a direct band gap of about 1.0 to 1.17eV, which makes it more desirable and efficient for applications. With a thickness of 3μm, it showed a high

open circuit voltage due to the back electrical field [Li, 2019]. However, the maximum desirable band gap is about 1.68eV [Ghavami, 2020]. It limits the number of incident photons that are photovoltaic solar absorbed by just a few micrometers. In order to fully absorb incident photons, the absorber layer must be thick enough. However, profound thickness degrades solar cell efficiency and ends up in material waste [Bendoumou, 2022]. The main purpose of this research is to analyze the efficiency of CIGS solar-cells by using solar simulation software called WxAMPS (Analysis of Microelectronic and Photonic Structures). The algorithm of this software computes the recombination profile of the steady-state band diagram, the one-dimensional transport of carriers based on the Poisson equation of electrons and holes. In this research work, the ZnO/CdS bilayer window is used to demonstrate that with a current density of 36.68 mA/cm^2, fill factor of 79.42%, the maximum QE achieved with 99% at 548 nm in the device, and the cell efficiency has been raised to 18.7%. To meet future demand, we are motivated to design and perform an analysis of CIGS Solar Cell using wxAMPS.

2. Mathematical Modeling & Simulation

There are several simulation software solutions, including Analysis of Microelectronic and Photonic Structures one Dimension (AMPS-1D) [Shakoor, 2023], wxAMPS (Analysis of Microelectronic and Photonic Structures, widgets provided) [Ying, 2022], Photovoltaic cell 1-Dimension (PC1D) [Hernandez-Como, 2010], and Solar Cell Capacitance Simulator in 1 Dimension (SCAPS-1D) [Jani, 2020] for thin film solar cells. This software has been created to investigate the operation of multilayer films of solar materials. We have performed numerical analysis utilizing wxAMPS, a free solar-cell simulation software. This simulation software is an improved version of the previous AMPS-1D software, which was developed by Fonash et al. at Pennsylvania State University. On top of that, it was rewritten in C++ by Rockett et al. (2012) at the University of Illinois [Soro, 2023]. The simulation of optical and electronic activity for a variety of solar cell system designs is enabled by wxAMPS. Different solar cell material model's structures can be easily designed using this software program. This simulation software explains numerical analysis that provides an in-depth description of a cell's physical activity. Furthermore, it is possible to assess the variation of certain material parameters that affect the solar cell. As a result, several parameters and characteristics, such as I-V curves, fill-factor, efficiency, energy band diagrams, electric field, carrier density, and generation and recombination velocity, can be easily and automatically computed. The versatility of wxAMPS has also helped us to thoroughly investigate the optical responses and electrical transport phenomena of imagined structures in our solar cells. A huge number of layers of any combination and composition can be built to replicate the cross-section of any possible device. Some sophisticated algorithms, like a combination of the Gummel and Newton methods, are employed here. The benefits include improved strength and robust convergence in cases where an intra-band tunneling model with low densities of defect states is needed to measure specific solutions [18]. Ultimately, wxAMPS allows users to select the environment and physical properties of each layer through a comprehensive and user-friendly graphical interface. The Engineering Wiki website of the University of Illinois provides an upstanding starting set of simulation parameters, but it is also possible to freely modify the database using worksheets [Parisi, 2015].

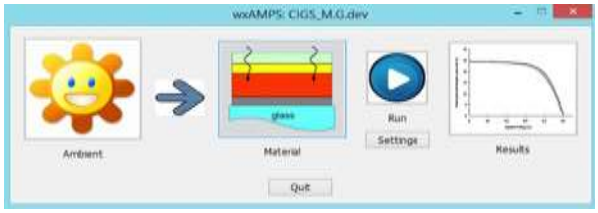

Fig. 1. Front panel of wxAMPS simulation software [Liu, 2011]

Some important equations that are solved using AMPS-1D simulation software (using finite differences and the Newton-Raphson technique) are [Omer, 2011]:

Poisson's equation:

$$\frac{d^2}{dx^2}\psi(x) = \frac{\rho(x)}{\varepsilon} \quad (1)$$

Electron continuity equation:

$$G_{op}(x) - R(x) - \frac{1}{q}\left(\frac{dJ_n}{dx}\right) = 0 \quad (2)$$

Hole continuity equation:

$$G_{OP}(x) - R(x) - \frac{1}{q}\left(\frac{dj_p}{dx}\right) = 0 \qquad (3)$$

Electron current density:

$$j_n(x) = q\mu_n n\left(\frac{dE_{fn}}{dx}\right) \qquad (4)$$

Hole current density:

$$j_p(x) = q\mu_p p\left(\frac{dE_{fp}}{dx}\right) \qquad (5)$$

The first equation (1) is the Poisson equation where ρ is the space charge density and given by:

$$\rho = q.[p(x) - n(x) + N_D^+(x) - N_A^-(x) + p_t(x) - (x)] \qquad (6)$$

In AMPS-1D software, the net recombination rate in terms of $R(x)$ in the continuity equations takes both the direct R_D and indirect recombination R_I into consideration,

$$\mathrm{R}(x) = R_D(x) + R_I(x) \qquad (7)$$

The net direct recombination rate is given by

$$R_D(x) = b_R(np - n_0p_0) \qquad (8)$$

Where b_R is the direct band-to-band recombination strength, n and p are the band carrier concentrations present when devices are subjected to a voltage bias, light bias, or both. n_0 (p_0) is the intrinsic electron (hole) density.

The Shockley-Read-Hall(S-R-H) net recombination trapping through each group of defects of density n_t is given by:

$$R_I(x) = \frac{(np - n_0p_0)}{\left(\tau_{po}(n+n_L) + \tau_{no}(p+p_L)\right)} \qquad (9)$$

The optical generation rate $G_{op}(x)$ is expressed as:

$$G_{OP}(x) = -\frac{d}{dx}\sum_i \varphi_i^{FOR}(\lambda_i, x) + \frac{d}{dx}\sum_i \varphi_i^{REV}(\lambda_i x) \qquad (10)$$

Where, ϕ_i^{FOR} and ϕ_i^{REV} are the photon flux of the incident light and reflected light from the back surface at a certain wavelength, respectively, λ_i at some point x that depends on the light reflection and absorption coefficient in the reverse and forward direction.

3. Device Structure and Material Parameters

In this analysis, a solar cell of ZnO: Al/ZnO/CdS/CIGS/Mo/substrate model is considered in Fig. 2. The CIGS absorber layer is the most essential layer with multiple materials (Copper, Indium, Gallium, Selenide) of the aforementioned photovoltaic cell. As in conventional CIGS solar cells, we considered a single absorber layer with constant properties (i.e., doping concentrations, band gap, dielectric constant, etc.) in our work.

CdS layer, the buffer layer, has a direct band gap of 2.4 eV that enhances solar cell efficiency by reducing the interface recombination, preventing the undesirable shunt paths through the absorber layer and allowing less structural damage due to the subsequent deposition of ZnO onto CIGS. Furthermore, since its refractive index is between those of ZnO and CIGS, the CdS layer decreases reflection losses at the cell surface. As shown in Fig. 2, the n-type ZnO-CdS and p-type CIGS form a p-n junction. CdS thickness is typically chosen in the 50-100 nm range because it is the best balance between the benefits described above and losses due to optical absorption. An n-doped ZnO and an aluminum-doped ZnO (ZnO: Al) layer are deposited on top of the buffer layer. The two transparent conductive oxide layers (TCO) have a broader band-gap transparent to the most solar spectrum. CIGS is a chalcopyrite compound semiconductor crystal structure that has a high absorption coefficient ($\alpha \sim 10^5\ \mathrm{cm}^{-2}$) [AMPS Modeling, n.d].

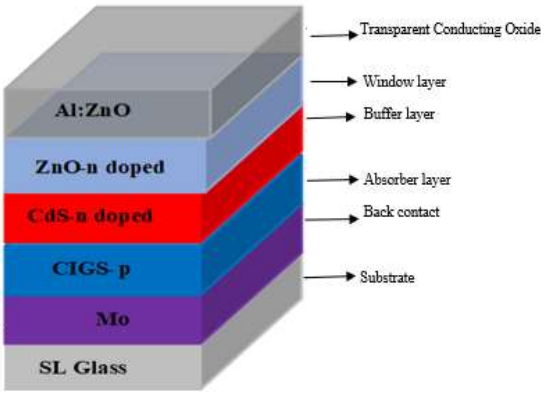

Fig. 2. CIGS solar cell layer structure.

The simulation software established the optical and electrical variables for each layer in Table 1 [Jehl, 2011; Al Ahmed, 2021; Scheer, 2011]. We looked at several band gap values and accompanied absorption spectra [Li, 2018].

TABLE I
Simulation material parameters of the CIGS thin-film
Solar cell

Layer Properties	ZnO-Al	ZnO	CdS	CIGS
Dielectric Constant	9	9	10	13.6
Electron Mobility (cm^2/Vs)	100	100	100	100
Hole Mobility (cm^2/Vs)	25	25	25	25
Carrier density (cm^{-3})	10^{18}	10^{18}	10^{17}	2×10^{6}
Band Gap (eV)	3.3	3.3	2.4	1.12
Effective Density (cm^{-3}) Nc	2.2×10^{18}	2.2×10^{18}	2.2×10^{18}	2.2×10^{18}
Effective Density (cm^{-3}) Nv	1.8×10^{19}	1.8×10^{19}	1.8×10^{19}	1.8×10^{19}
Electron affinity (eV)	4.0	4.0	3.8	4.1
Thickness (nm)	200	200	50	3000

According to the following equation, the absorber's band gap increases from 1.04 eV (pure CIS) to 1.69 eV (pure CGS) [Chakma, 2021]:

$$E_g = 0.244x^2 + 0.421x + 1.02 \quad (11)$$

Numerical simulations were performed using the standard AM1.5G solar spectrum, where on the top of the cell the reflection coefficient of 5% and a cell temperature of 300 K. Metal-to-semiconductor contacts, in general, can function as either a rectifying (Schottky) or an ohmic contact, depending on the interface properties. In particular, an ohmic metal/semiconductor contact is obtained in a p-type semiconductor with a band gap. E_g, electron affinity χ, and a metal with work function (φ) When

$$\Phi_m > E_g + \chi \qquad (12)$$

A rectifying contact, on the other hand, is produced when the following relationship occurs:

$$\Phi_m < E_g + \chi \qquad (13)$$

The majority of carriers (holes) encounter a barrier as they pass from the semiconductor to the metal at the Schottky-contact interface, but such a barrier does not exist at an ohmic contact interface. On the other hand, most of the metals do not have enough work functions, and hence, Schottky-barrier contacts are formed; this case is for the p-CIGS absorber layers/Molybdenum interface.

In the absence of surface states and in the situation of an ideal contact between a metal and a p-type semiconductor, the contact barrier height for holes can be expressed as follows [Hirai, 2013]:

$$\Phi_B = E_g + \chi - \Phi_m \qquad (14)$$

We have carried out the simulation by varying E_g, we have assumed $E_g + \chi$ is constant and equals to 5.55 eV [Ranade, 2001], and also φ_m (Mo) = 4.95 eV [Scheer, 2011], obtaining Φ_B=0.6eV. In other words, our simulations were performed keeping constant the back-contact barrier (Φ_B).

This causes substantial absorption of blue photons in the solar spectrum, as well as a quasi-conduction band offset that impedes photocurrent. To minimize absorption losses, CdS is embedded in a very thin layer. On top of the CdS layer, a highly resistive and highly transmissive ZnO (window layer) is deposited.

Filling pinholes in thin CdS could result in ZnO/CIGS diodes being formed in parallel with the CdS/CIGS junction, as well as adding a layer of protection from the sputtering process. A transparent conducting oxide (TCO) layer of doped ZnO or In_2O_3:Sn (ITO) is deposited to facilitate lateral current collection. Filling pinholes in thin CdS could lead to ZnO/CIGS diodes being formed in parallel with the CdS/CIGS junction, as well as adding a layer of protection from the sputtering process. To facilitate the lateral current array, a transparent conducting oxide (TCO) layer of doped ZnO or In_2O_3:Sn (ITO) is deposited. As a top gate using photolithography or evaporation with an aperture mask, the proposed cell is finally finished with aluminum metal. In brief, the proposed cell layer structure is as follows: ZnO window layer, CdS buffer layer, CIGS absorber layer, and Mo back contact layer. The layers of the cell are formed on a soda lime (SL) glass substrate.

4. Simulation Results and Discussion

4.1 I-V Curve of CIGS Solar Cell

Fig. 3 shows CIGS proposed model thickness dependent efficiency. The short circuit current density J_{sc} and open circuit voltage V_{oc} values are 36.68 $mA/\ cm^2$and 0.64V, respectively. The resulting fill factor (FF) is about 79.42%. The shunt resistance(R_{sh}) and series resistance (R_{sr}) values are found to be 701.8 $\Omega - cm^2$ and 0.03588$\Omega - cm^2$, respectively. The estimated value for cell efficiency is 18.7%. Here, the absorber thickness is taken at about 3000 *nm*. Other material parameters are given in Table 1. Experimentally, there is a significant power loss caused by the presence of shunt resistance due to manufacturing faults. For light generated current, power losses in solar cells due to low shunt resistance provide an alternate current path. Shunt resistance has an effect on solar cell efficiency. In our scenario, the second reason may be dominating and has an impact on FF. [FF=P_{MP}/ ($V_{oc}\times J_{sc}$)= ($V_{MP}\times J_{MP}$)/ ($V_{oc}\times J_{sc}$)] and finally efficiency [η= ($V_{oc}\times J_{sc}\times$FF)/ P_{in}] of the cell.

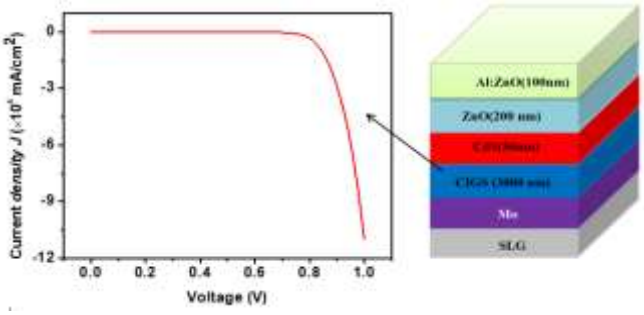

Fig. 3. Current-voltage (I-V) curve of the CIGS cell structure

4.2 Analysis on Band Diagram

Fig-4 depicts the energy band diagram of ZnO: Al/ZnO/CdS/CIGS/Mo/substrate solar structure at 300 K temperature in the 1.5 AM spectrum. The CIGS ultra-thin solar cell recompenses for back surface recombination in the conduction band (0.2μm) by producing a spike as well as near the back-contact field, a quasi ohmic contact by bending the valence band. The energy conversion efficiency is improved due to the characteristics of the low back surface recombination and quasi ohmic contact.

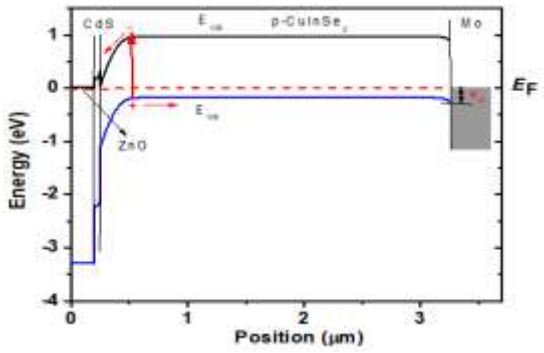

Fig. 4. Band diagram of CIGS solar cell under 1.5 AM spectrum.

4.3 Free Electron and Hole

The concentration of free electrons and holes in the cell structure is demonstrated in Fig. 5. It is worth noting that free electrons are only available in the ZnO layer, which is the window layer, and the CdS layer, which is the buffer layer, while free holes are available in the p-type CIGS region. It is clear that recombination between electron and hole is negligible in the system field, which increases cell efficiency. In a very narrow region, carrier generation is one order higher than recombination. However, generation is comparatively higher in a broad region, and the effective absorber region of CIGS is illustrated in Fig. 6.

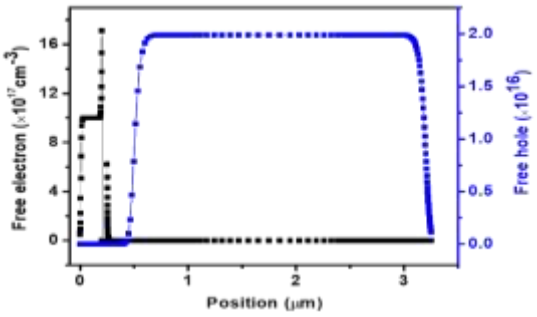

Fig. 5. Free electron and hole as a function of device thickness measured at room temperature (300 K)

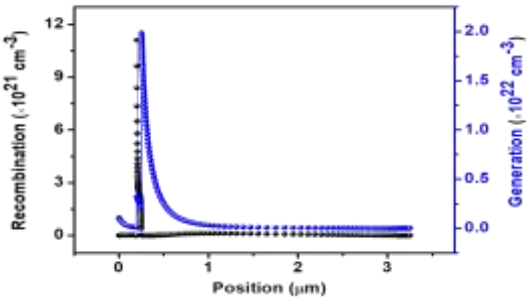

Fig. 6. Recombination and generation of carriers as a function of device thickness measured at room temperature (300 K)

4.4 Charge Donor & Acceptor Generation in Optimal Solar Cell

The device's charge acceptor and charge donor have been measured and illustrated in Fig. 7. In the conduction band, more electrons are accumulated and contribute to the flow current in the system, increasing cell performance.

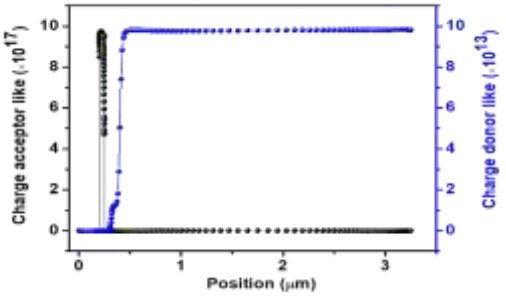

Fig. 7. Charge donor & acceptor generation in the optimal solar cell.

4.5 Electric Field of the CdS-CIGS Interface in the Proposed CIGS Solar Cell Structure

Fig. 8 illustrates the electric field that is computed at the CdS-CIGS interface. Only at the CdS-CIGS interface there appears an electric field, which is caused by the band of the p-type CIGS semiconductor material used to align the Fermi level. There is no region within the device other than the electric field that is good for carrier transport to the electrodes or for efficiency.

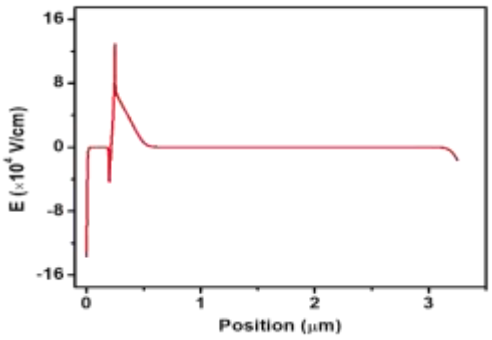

Fig. 8. Electric field of the CdS-CIGS interface

4.6 Electron, Hole, and Total Current Density of CIGS Solar Cell Structure

In Fig.9, the current density for electron (J_n), hole (J_p) and total (J_{total}) in the stacked system is shown. The $J_n$decreases rapidly as the device thickness increases, while the J_p increases steadily and remains constant. The J_{total} remains almost constant and still maintains specific values.

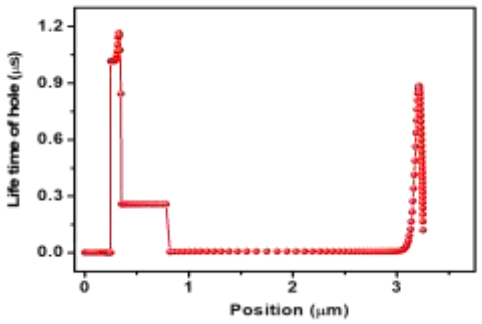

Fig. 9. Electron, hole, and total current density of CIGS solar cell structure

4.7 Life Time of Minority Carriers in the CIGS Solar Cell Structure

Minority carrier life times are measured as a function of layer thickness in the device, which is depicted in Fig. 10. The shorter life cycle of the minority carrier is beneficial to system performance. The life time of minority holes in CdS is found to be 1.1 μs, which is fair in the range, and it is in a very short field. Minority carrier electrons have a life time of 0.25 μs in the p-type CIGS field, which decreases to zero after 0.78 μs.

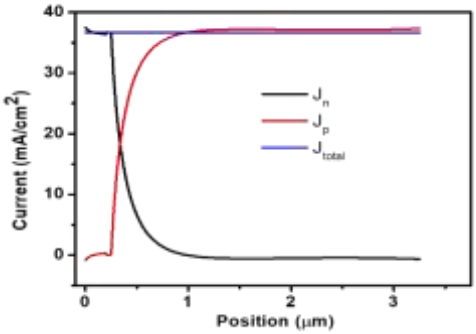

Fig. 10. Life time of minority carriers in the CIGS solar cell structure

4.8 Quantum Efficiency

"Quantum Efficiency" (Q.E.) is the quantitative relation of the quantity of carriers collected by the photovoltaic cell to the quantity of photons of a given energy incident on the photovoltaic cell. Quantum efficiency is unity at a particular wavelength when certain wavelength's photons are absorbed, and the resulting minority carriers are collected. Quantum efficiency is zero when the energy of the photon is below the band gap. Ideally, quantum efficiency has a square shape due to the effects of recombination; most solar cells' quantum efficiency is reduced.

The calculated quantum efficiency (QE) has been shown in Fig. 11. The dominant factor in our device is the front surface recombination and low diffusion length. The maximum QE is achieved with 99% at 548 nm in the device.

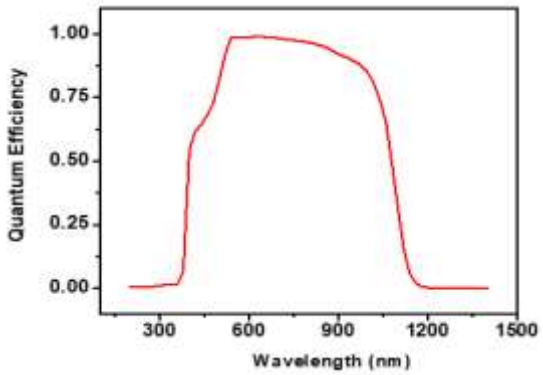

Fig. 11. Quantum efficiency of CIGS solar cell.

4.9 Temperature Effect on the Efficiency of the Cell

All semiconductor devices are temperature sensitive. An increase in temperature minimizes the band gap of a semiconductor, which affects the majority of the semiconductor material parameters. Reducing the semiconductor's band gap with increasing temperature can be interpreted as an energy rise of the electrons in the material. As a result, less energy is required to break the bond. Reduced bond energy eliminates the band gap in the bond model of a semiconductor band gap. As a result, increasing the temperature decreases the band gap.

The open-circuit voltage is the parameter mostly influenced by temperature change in a solar cell. The effect of rising temperatures is depicted in the graph below. The following figure depicts the influence of temperature on the IV characteristics of a solar cell:

The calculated efficiency of the cell as a function of temperature is shown in Fig. 12. It has already been discussed that rising temperature reduces the band gap of the semiconductor, which gives better cell efficiency.

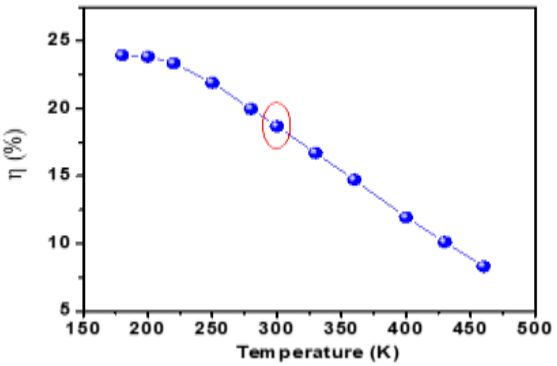

Fig. 12. Temperature dependent efficiency of the cell.

In contrast to studies that enhance CIGS solar cell efficiency by introducing new absorber layers such as InGaAs and AlGaAs, which achieve up to 28% efficiency [Merad, 2020], our research focuses on simulating the performance of the ZnO/ZnO/CdS/CIGS/Mo structure using WxAMPS software. This method investigates the effect of varying absorber thicknesses and band gaps without introducing alternative absorber materials, resulting in a maximum efficiency of 18.7%.

This study does not address the long-term stability or potential degradation of CIGS solar cells when exposed to varying environmental conditions such as temperature and humidity. Additionally, it does not explore the practical challenges associated with scaling up the proposed design for mass production, including considerations of manufacturing complexity and cost.

5. Conclusion

Analyzing the result using solar simulation software wxAMPS, the efficiency of the cell ZnO: Al/ZnO/CdS/CIGS/Mo/substrate obtained is about 18.7% at 300K temperature under 1.5 AM spectrum. In the device, a quasi electrical field directed toward the back-contact is induced through the absorber, conduction band, and valence band; energy increases towards the back-contact, and thus, the energy gap remains constant along the depth. Therefore, the generation process is more efficient in CIGS cells. The observations are important for sustainable experimental work since they will allow for technical optimization. Investigating various combinations of buffer layers and window layers by varying their thickness and examining the long-term effects of temperature fluctuations on the performance of CIGS solar cells, particularly under different environmental conditions, could enhance thermal stability and overall efficiency.

Acknowledgment: This work was supported in part by the Department of Electrical and Electronic Engineering of the University of Science and Technology Chittagong, Bangladesh. Special thanks to Sheikh S. Mahtab, PhD candidate in Electrical Engineering at Morgan State University, Baltimore, United States, for his valuable contributions.

References

[1] Al-Ahmed SR, Sunny A, and Rahman S. (2021). Performance enhancement of Sb2Se3 solar cell using a back surface field layer: a numerical simulation approach. Solar Energy Materials and Solar Cells. 2021 Mar 1;221:110919.

[2] Ahamed E. M. K. I., Matin M. A., and Amin N. (2017). Modeling and simulation of highly efficient ultra-thin CIGS solar cell with MoSe2 tunnel, *2017 4th International Conference on Advances in Electrical Engineering (ICAEE)*, 2017, 681-685.

[3] Antonino P, Riccardo P, Vincenzo R and Luciano C, (2015). Graded Carrier Concentration Absorber Profile for High Efficiency CIGS Solar Cells, *Hindawi Publishing Corporation International Journal of Photoenergy* 2015, Article ID 410549, 9 pages.

[4] AMPS Modeling, (n.d).AMPS modeling, [Online]. Available: http://www.ampsmodeling.org/latest.html.

[5] Bendoumou, A, Abderrahim R, Atika F, Mohamed L, and Mounir F. (2022) Numerical Simulation: Toward High-Efficiency CIGS Solar Cell Through Buffer Layer Replacement. In International Conference on Electronic Engineering and Renewable Energy Systems, 139-150. Singapore: Springer Nature Singapore, 2022.

[6] Columbus, D A. (2014) Design and optimization of copper indium gallium selenide solar cells for lightweight battlefield application. PhD diss., Monterey, California: Naval Postgraduate School, 2014.

[7] Chakma, R., Mahtab, S.S., Alam, M.J., Akter, R. (2021) Design and Performance Analysis of GaAs-Based P-i-N Photovoltaic Using AlGaAs as Window Layer, In: Bindhu, V., Tavares, J.M.R.S., Boulogeorgos, AA.A., Vuppalapati, C. (eds) International Conference on Communication, Computing and Electronics Systems. Lecture Notes in Electrical Engineering, 733. Springer, Singapore. https://doi.org/10.1007/978-981-33-4909-4_19.

[8] Ghavami, F, and Alireza, S. (2020) High-efficiency CIGS solar cell by optimization of doping concentration, thickness, and energy band gap. Modern Physics Letters B 34, 04 (2020): 2050053.

[9] Global Solar Energy Share Electricity. (n.d) [Online]. Available: https://www.statista.com/statistics/1302055/global-solar-energy-share-electricity-mix/

[10] Hirai, Y, Yasuyoshi K, and Akira Y. (2013) Numerical study of Cu (In, Ga) Se2 solar cell performance toward 23% conversion efficiency. *Japanese Journal of Applied Physics* 53, 1 (2013): 012301.

[11] Hernandez-Como, N, and Arturo M. (2010) Simulation of hetero-junction silicon solar cells with AMPS-1D. Solar Energy Materials and Solar Cells 94, 1 (2010): 62-67

[12] Jehl, Z., F. Erfurth, N. Naghavi, L. Lombez, I. Gerard, M. Bouttemy, P. T. (2011) Thinning of CIGS solar cells: Part II: Cell characterizations. Thin solid films 519, no. 21 (2011): 7212-7215

[13] Jani Md R., Islam Md T., Amin S. M. Al, Sami Md S. U., Shorowordi K. M., Hossain M. I., Chowdhury S., Nishat S. S., and Ahmed S. (2020) Exploring solar cell performance of inorganic Cs_2TiBr_6 halide double perovskite: A numerical study, Superlattices and Microstructures, 146, 106652, 2020.

[14] Li, H, Fei Q, Haitian L, Xiaona N, Jingwei C, Yi Z, Huijun Y, Xiaojie J, Hongwei G, and Wenjing W. (2019) Engineering CIGS grains qualities to achieve high efficiency in ultrathin Cu (InxGa1− x) Se2 solar cells with a single-gradient band gap profile. Results in Physics 12 (2019): 704-711.

[15] Liu Y., Sun Y., and Rockett, A. (2012). An improved algorithm for solving equations for intra-band tunneling current in heterojunction solar cells, Thin Solid Films, 520, 15, 4947– 4950, 2012.

[16] Liu, Y, Dan H, and Angus R. (2011). A new solar cell simulator: WxAMPS. In 2011 37th IEEE Photovoltaic Specialists Conference, 002753-002756.

[17] Li, J., Wang, D., Li, X., Zeng, Y., & Zhang, Y. (2018). Cation substitution in earth-abundant kesterite photovoltaic materials. Advanced Science, 5(4), 1700744.

[18] Merad, F., Guen-Bouazza, A., Kanoun, A.A., & Merad, A.E. (2020) Optimization of Ultra-Thin CIGS Based Solar Cells by Adding New Absorber Layers: InGaAs and AlGaAs. Springer Proceedings in Energy, ICREEC 2019. Springer, Singapore, 2020.

[19] Omer, B M, Ahmed K, and Almantas P. (2011) AMPS-1D modeling of P3HT/PCBM bulk-heterojunction solar cell. In 2011 37th IEEE photovoltaic specialists conference, 000734-000743. IEEE, 2011.

[20] Parisi, A., Riccardo P., Vincenzo R, Luciano C, Salvatore S, Alfonso C. C, and Giovanni C, et al. (2015) Graded carrier concentration absorber profile for high efficiency CIGS solar cells. *International Journal of photoenergy* 2015, 1 (2015): 410549

[21] Ranade, P, Hideki T, Tsu-Jae K, and Chenming H. (2001) Work function engineering of molybdenum gate electrodes by nitrogen implantation. Electrochemical and Solid-State Letters 4, 11 (2001): G85

[22] Scheer R., (2011) Towards an electronic model for 8 CuIn1-xGaxSe2 solar cells, Thin Solid Films, 519, 21, 7472–7475,2011.

[23] Solar Electric Technology, (n.d) Solar electric technologies, Energypedia, [Online].

[24] Solar Reviews (n.d) How do solar cell work [Online]. Available: https://www.solarreviews.com/blog/thin-filmsolar-panels.

[25] Soro, D. , Toure, S. , Sylla, A. , Bouich, A. , Mari-Guaita, J. , Toure, S. and Soucase, B. (2023) Numerical Simulation of Tandem Using ZnS as a Buffer Layer Cu I(1-x) CaxSe2/CuGaSe2. Modeling and Numerical Simulation of Material Science, 13, 1-10.

[26] Shakoor A. (2023). Performance Evaluation of Solar Cells by Different Simulating Softwares, Solar PV Panels - Recent Advances and Future Prospects. IntechOpen, Sep. 06, 2023. doi: 10.5772/intechopen.111639.

[27] Scheer, R. (2011). Towards an electronic model for CuIn1− xGaxSe2 solar cells. Thin Solid Films 519, no. 21 (2011): 7472-7475.

[28] Thin-film Solar Cell, (n.d). Thin-film solar cell, Britannica, [Online].

[29] Thin film solar stuck in second place even with csi-tariffs.[Online]. (2018) Available: https://www.solarpowerworldonline.com/2018/07/thin-film-solar-stuck-in-second-place-even-with-c-si-tariffs/

[30] Witte W., Powalla M., and Hariskos D., (2012). Chemical gradients in Cu(In, Ga)(S, Se)2 thin-film solar cells: results of the GRACIS project, In progess of the 27th European Photovoltaic Solar Energy Conference and Exhibition, 2166-2173, G ermany, 2012.

[31] Ying, M, Junjie W, and Yue Z. (2022). Numerical simulation of CuInSe2 solar cells using wxAMPS software. *Chinese Journal of Physics 76* (2022): 24-34.